Electronic Supplementary Material (ESI) for CrystEngComm.

Versatile solid forms of boscalid: insight into the crystal structures and phase transformations

Zhonghua Li[a], Lina Jia[a], Peng Shi[a], Shuang Jiang[a], Junbo Gong[a, b], Songgu Wu[*, a, b]

a. State Key Laboratory of Chemical Engineering, School of Chemical Engineering and Technology, Tianjin University, Tianjin 300072, P. R. China.

b. Key Laboratory Modern Drug Delivery and High Efficiency in Tianjin University, P. R. China.

Contents of Supporting Information

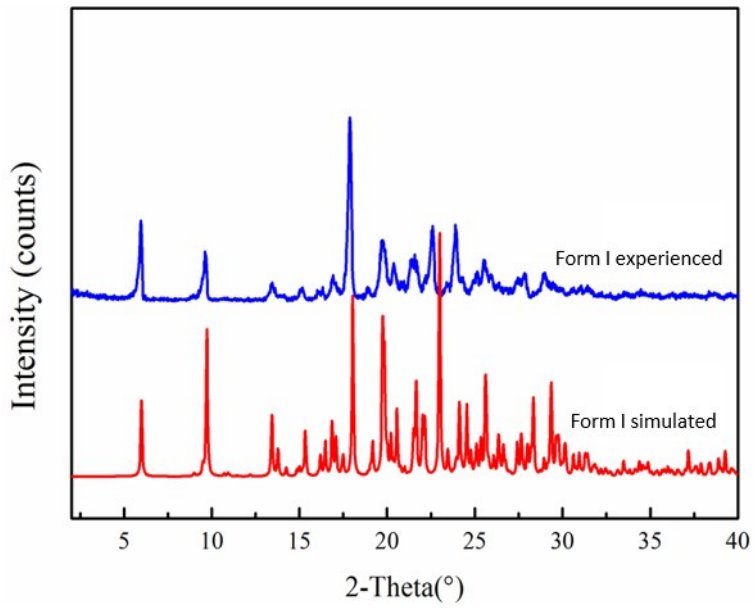

Fig. S1 Experimental and calculated powder X-ray diffraction patterns of form I.

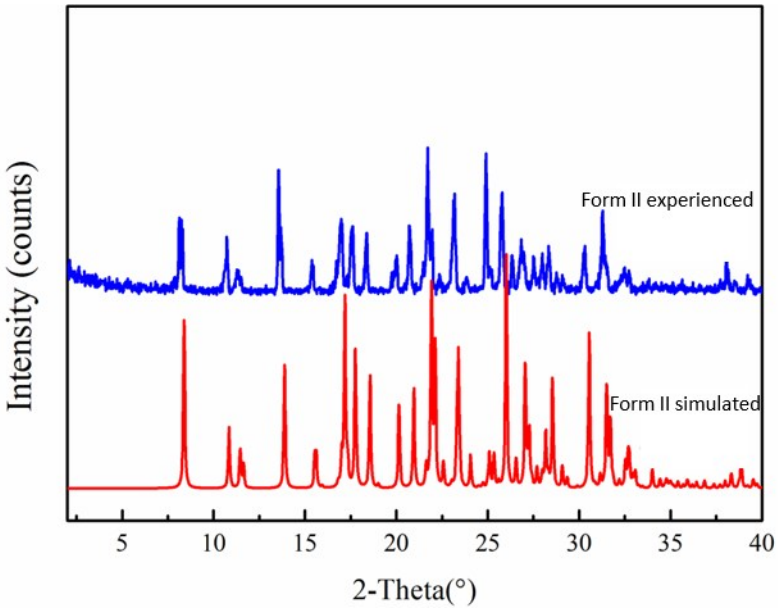

Fig. S2 Experimental and calculated powder X-ray diffraction patterns of form II.

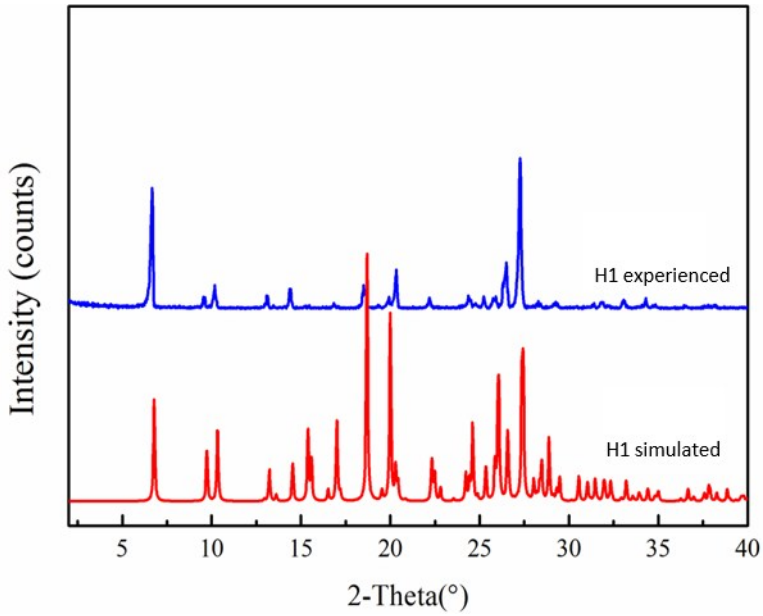

Fig. S3 Experimental and calculated powder X-ray diffraction patterns of H1.

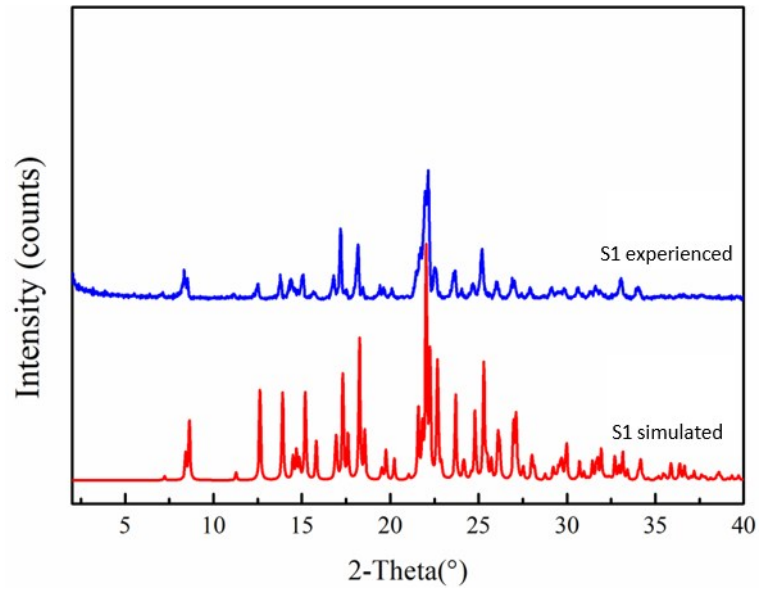

Fig. S4 Experimental and calculated powder X-ray diffraction patterns of S1.

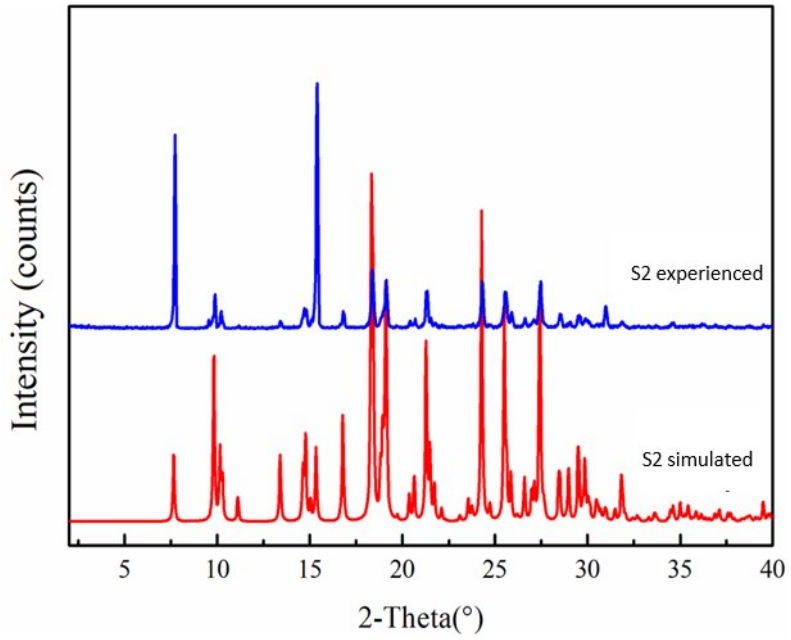

Fig. S5 Experimental and calculated powder X-ray diffraction patterns of S2.

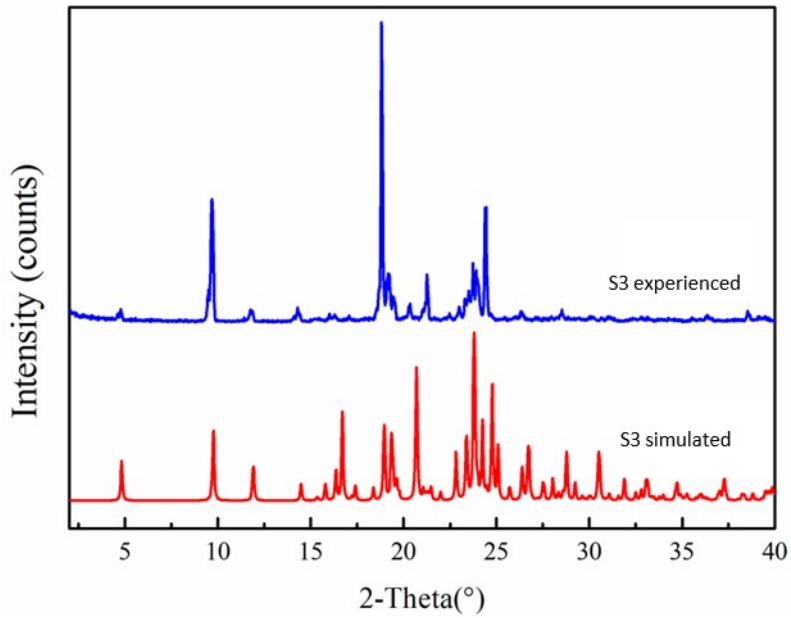

Fig.S6 Experimental and calculated powder X-ray diffraction patterns of S3.

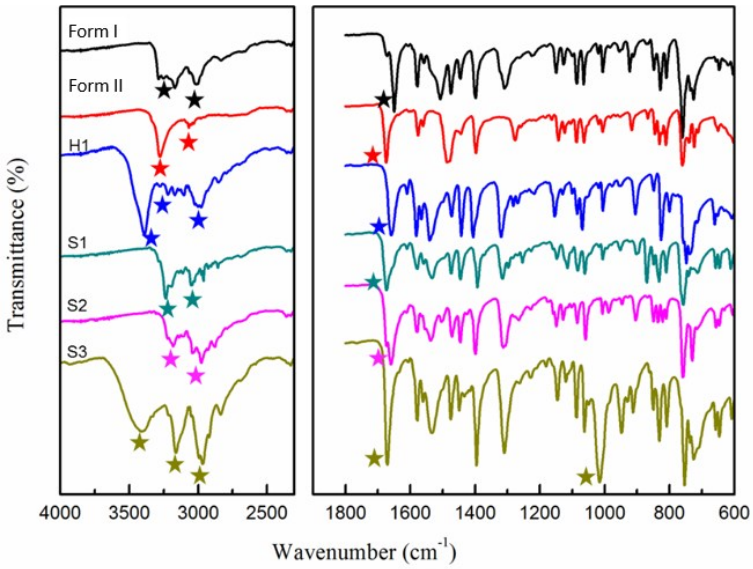

Fig. S7 FT-IR spectrum of different forms of boscalid.

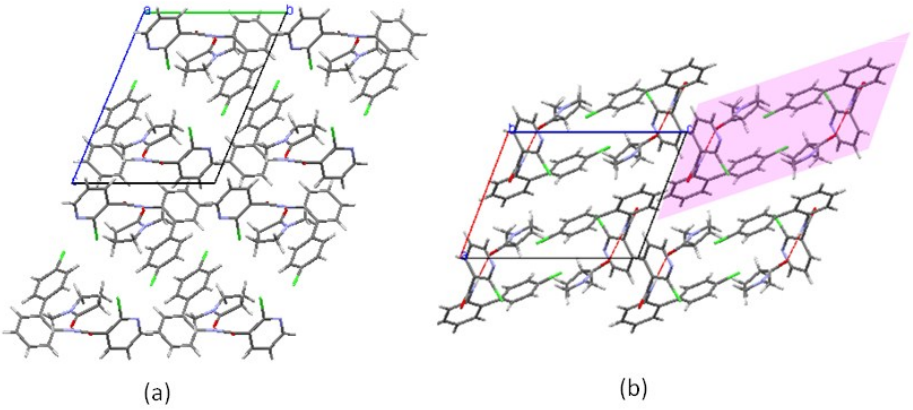

Fig. S8 (a) Molecular packing network inside the b-c plane for S2, (b) Molecular packing network inside the a-c plane for S2.

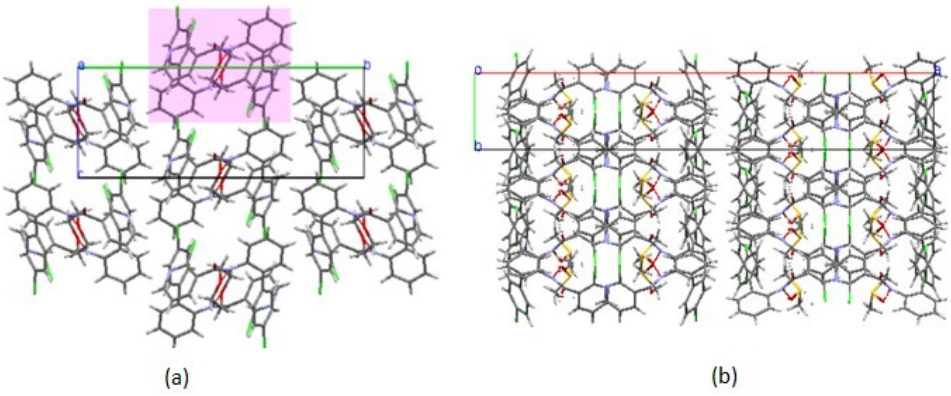

Fig. S9 (a) Molecular packing network inside the b-c plane for S1, (b) Molecular packing network inside the a-b plane for S3.

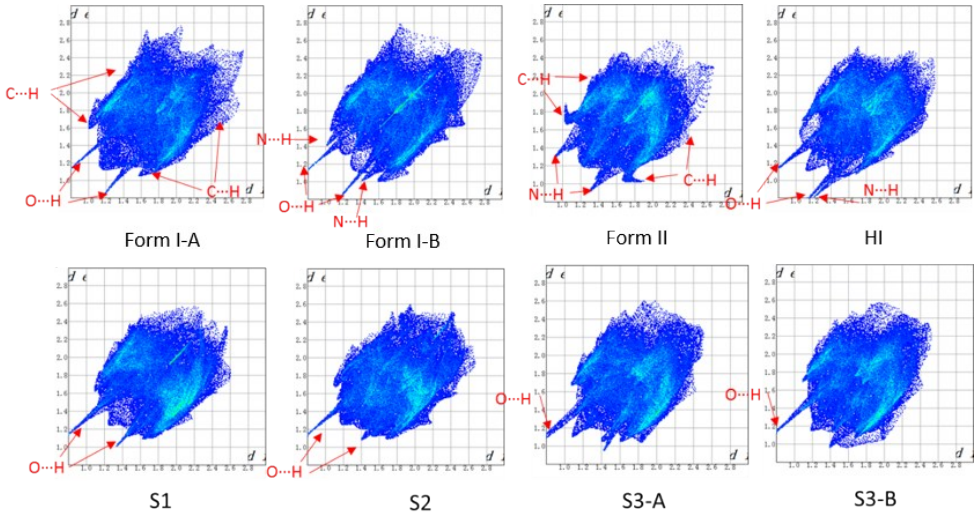

Fig. S10 2D fingerprint plots of different solid forms.

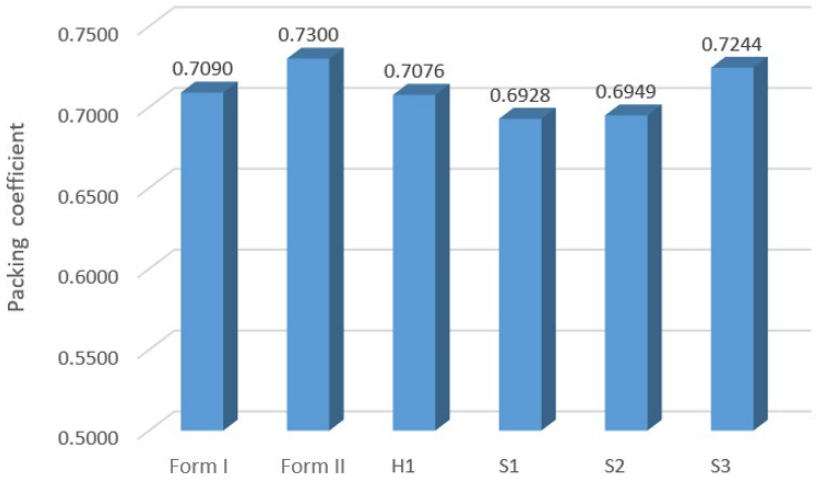

Fig. S11 Packing coefficient of boscalid forms.

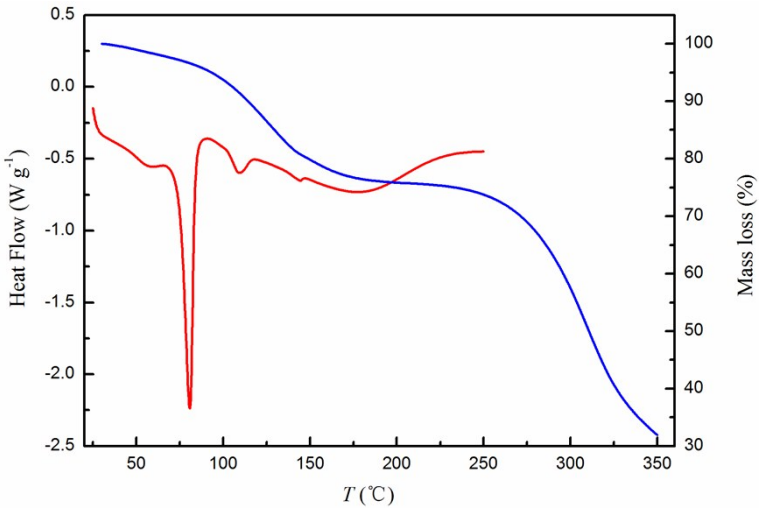

Fig. S12 DSC/TGA curves of S3.

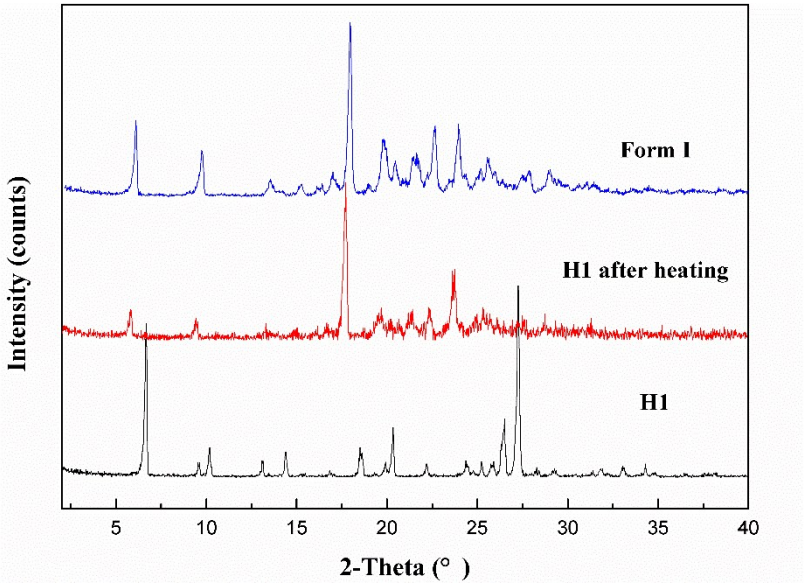

Fig.S13 Compared powder X-ray diffraction patterns of H1 before and after dehydration.

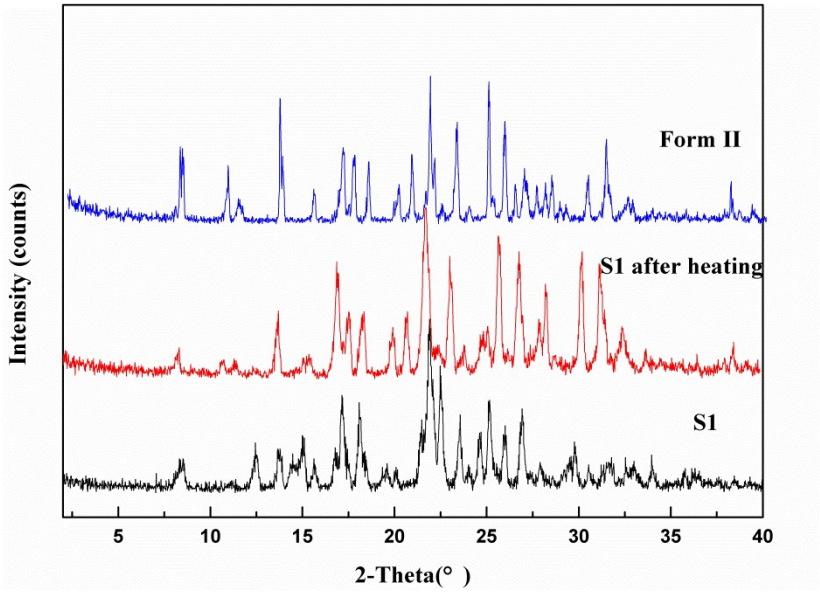

Fig. S14 Compared powder X-ray diffraction patterns of S1 before and after desolvation.

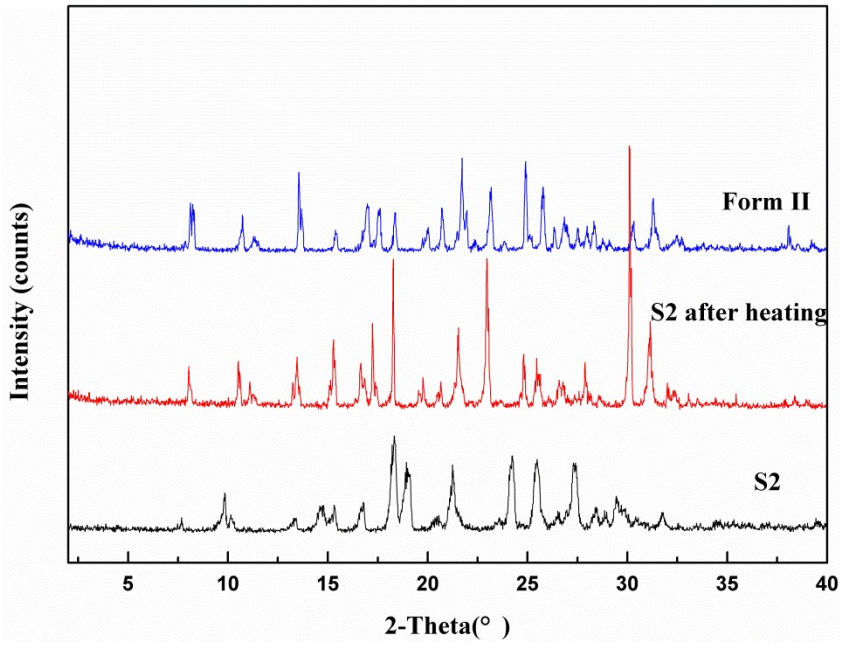

Fig. S15 Compared powder X-ray diffraction patterns of S2 before and after desolvation.

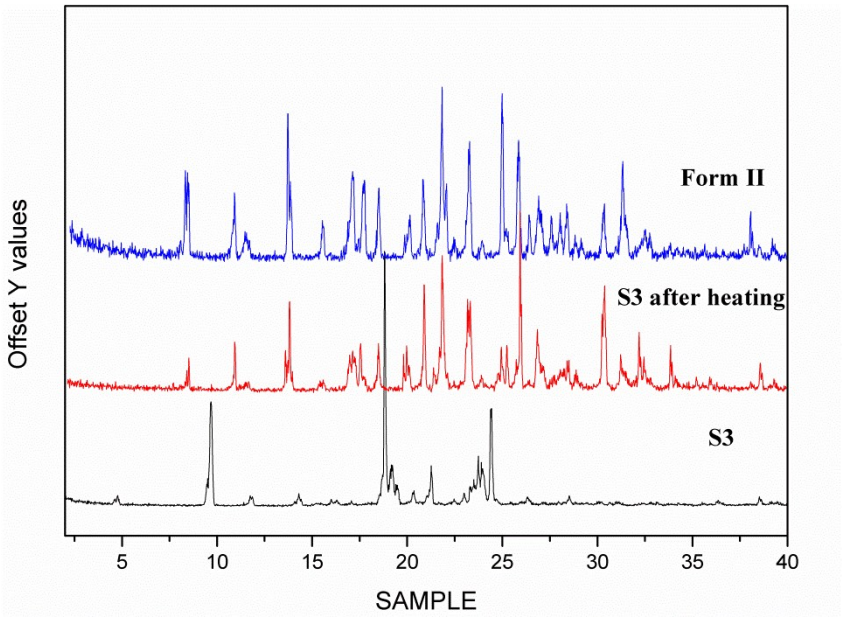

Fig. S16 Compared powder X-ray diffraction patterns of S3 before and after desolvation.

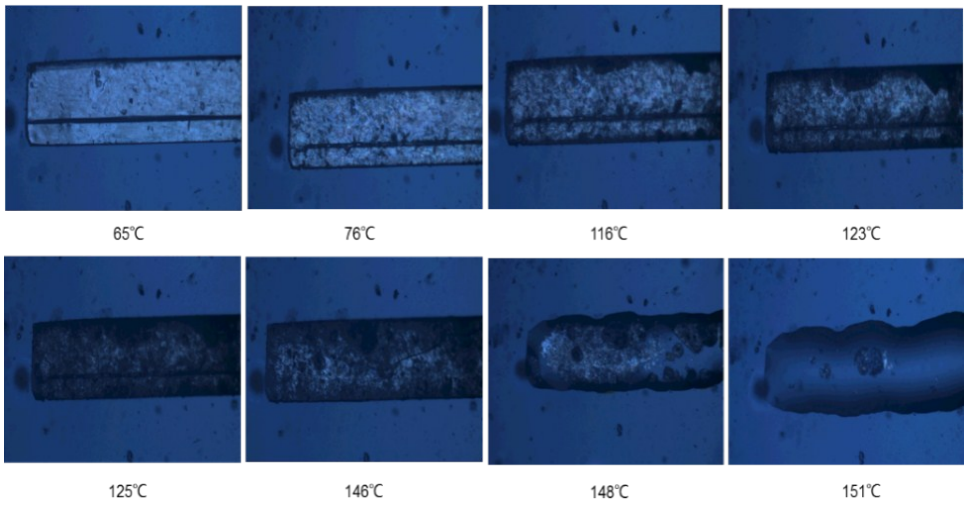

Fig. S17 HSM images of H1.

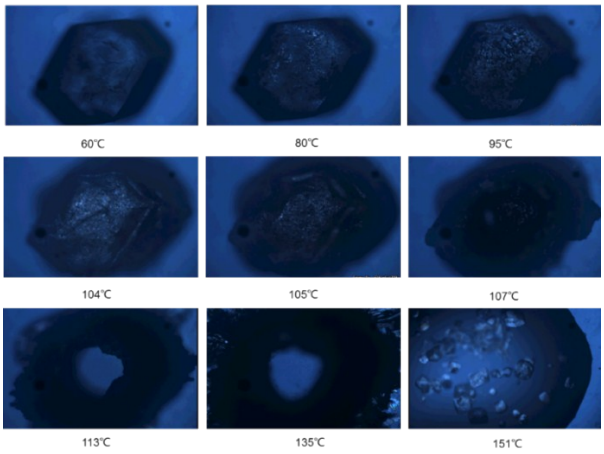

Fig. S18 HSM images of S2.

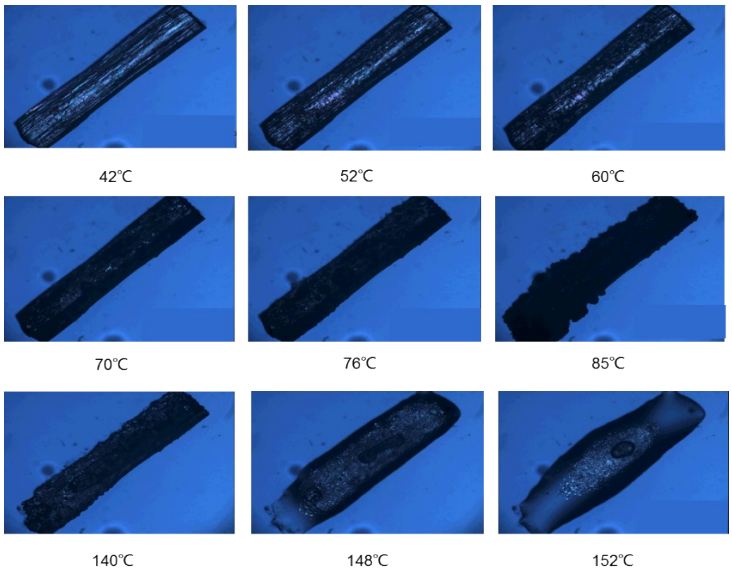

Fig. S19 HSM images of S3.

■ **Stability studies of solid forms of boscalid.**

Accelerated stability tests: the stability of boscalid solid forms was investigated at 40℃ and 75% relative humidity (RH) for 15 days due to time constraints. 75% RH was achieved with saturated sodium chloride solution in a desiccator. Fig. S20a and Fig. S20b displayed the PXRD patterns of the boscalid solid forms, which were monitored at 40℃ and 75% RH. All of the solid forms except H1 showed good stability because their PXRD patterns were nearly unchanged for 15 days. However, H1 was converted to form I within 7 days.

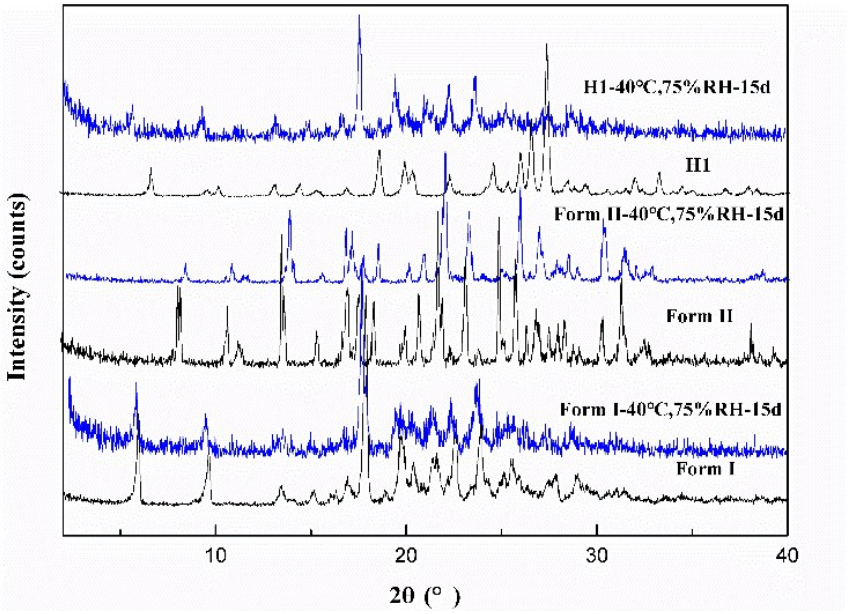

Fig. S20a Stability of form I, form II and H1 monitored with PXRD at 40 ℃, 75% RH. (d =day)

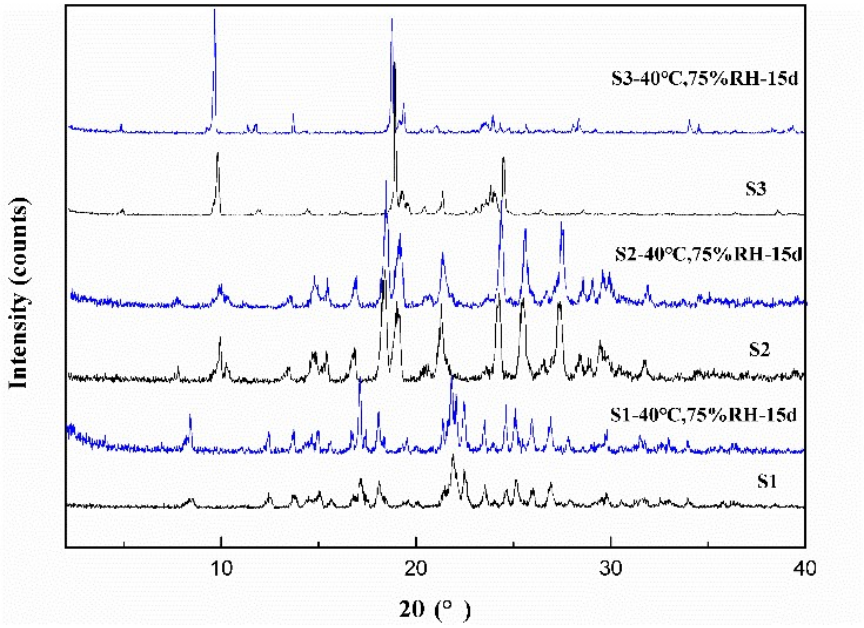

Fig. S20b Stability of S1, S2 and S3 monitored with PXRD at 40 ℃ and 75% RH. (d =day)

Liquid assisted grinding (LAG) experiments: the LAG experiments at room temperature was carried out on boscalid solid forms up to 30min to gain an insight into the stability of crystal forms under mechanical action. During the experiment, we added 2 drops of water to assist grinding to explore whether the solid forms are sensitive to humidity. The experimental results proved that mechanical action did not show any effect on form I, form II, H1, S1 and S2 (Fig. S21a and S21b). However, S3 was converted to H1 after the LAG experiments.

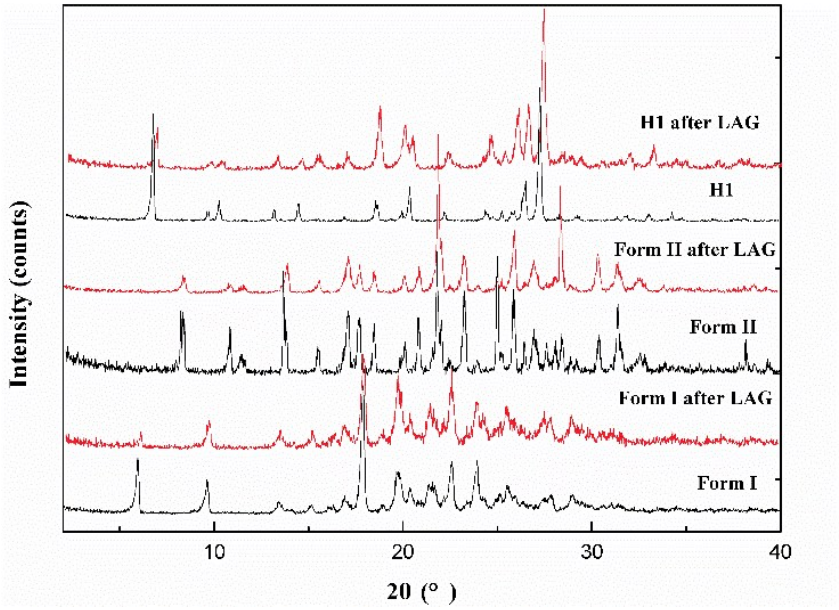

Fig. S21a Stability of form I, form II and H1 monitored with PXRD after LAG experiments.

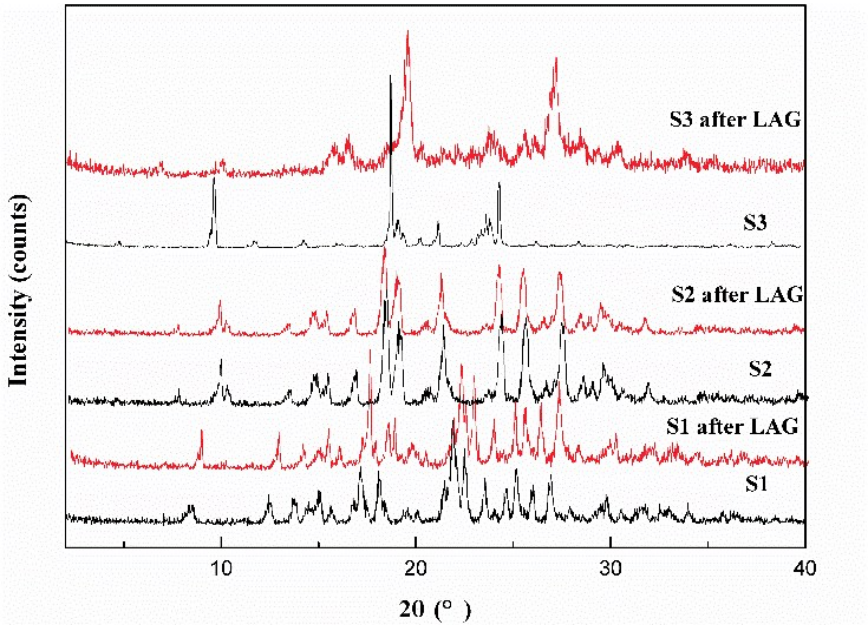

Fig. S21b Stability of S1, S2 and S3 monitored with PXRD after LAG experiments.

Dynamic vapour sorption (DVS) tests: Stability of the boscalid solid forms with respect to changes in relative humidity was evaluated by DVS experiments. Samples

of form I, form II, H1, S1, S2 and S3 exhibited low absorption (<1%) even at higher RH (>90%). In addition, their absorption and desorption profiles essentially overlap suggesting that the absorption and desorption profiles are reversible. The DVS tests showed that boscalid solid forms products were insensitive to humidity.

Table S1 Hydrogen bonds in crystal structures of solid forms of boscalid.

	D-H···A	d(D-H)，Å	d(H···A)，Å	d(D-A)，Å	∠(DHA)，deg.
Form I	N_1'-H···O_1	0.888	1.924	2.809	173.69
Form II	N_1-H···N_2	0.859	2.322	3.063	144.60
H1	O_{w1}-H···O_1	0.886	1.862	2.749	174.68
	O_{w1}-H···N_2	1.063	1.954	2.976	160.12
	N_1-H···O_{w1}	0.860	2.017	2.852	163.45
S1	N_1-H···O_2	0.860	1.995	2.843	168.72
S2	N_1-H···O_2	0.860	1.963	2.819	173.29
S3	N_1'-H···O_2	0.880	1.913	2.785	170.83
	N_1-H···O_2'	0.890	1.910	2.719	169.76